Available online at www.sciencedirect.com
ScienceDirect
Geomorphology 78 (2006) 265–278
GEOMORPHOLOGY
www.elsevier.com/locate/geomorph

Longevity and progressive abandonment of the Rocky Flats surface, Front Range, Colorado

Catherine A. Riihimaki [a,*], Robert S. Anderson [b,c], Elizabeth B. Safran [d], David P. Dethier [e], Robert C. Finkel [f], Paul R. Bierman [g]

[a] Department of Geology, Bryn Mawr College, 101 N. Merion Ave., Bryn Mawr, PA 19010, USA
[b] INSTAAR, University of Colorado, Campus Box 450, Boulder, CO 80309, USA
[c] Department of Geological Sciences, University of Colorado, Campus Box 399, Boulder, CO 80309, USA
[d] Environmental Studies Program, Lewis and Clark College, 0615 S.W. Palatine Hill Rd., Portland, OR 97219, USA
[e] Department of Geosciences, Williams College, Williamstown, MA 01267, USA
[f] Center for Accelerator Mass Spectrometry, Lawrence Livermore National Laboratory, MS L-206, 7000 East Ave, Livermore, CA 94550-9234, USA
[g] Geology Department, University of Vermont, Burlington, VT 05405, USA

Received 4 August 2005; received in revised form 23 January 2006; accepted 24 January 2006
Available online 6 March 2006

Abstract

The post-orogenic evolution of the Laramide landscape of the western U.S. has been characterized by late Cenozoic channel incision of basins and their adjacent ranges. One means of constraining the incision history of basins is dating the remnants of gravel-capped surfaces above modern streams. Here, we focus on an extensive remnant of the Rocky Flats surface between Golden and Boulder, Colorado, and use in situ-produced ^{10}Be and ^{26}Al concentrations in terrace alluvium to constrain the Quaternary history of this surface. Coal and Ralston Creeks, both tributaries of the South Platte River, abandoned the Rocky Flats surface and formed the Verdos and Slocum pediments, which are cut into Cretaceous bedrock between Rocky Flats and the modern stream elevations. Rocky Flats alluvium ranges widely in age, from >2 Ma to ~400 ka, with oldest ages to the east and younger ages closer to the mountain front. Numerical modeling of isotope concentration depth profiles suggests that individual sites have experienced multiple resurfacing events. Preliminary results indicate that Verdos and Slocum alluvium along Ralston Creek, which is slightly larger than Coal Creek, is several hundred thousand years old. Fluvial incision into these surfaces appears therefore to progress headward in response to downcutting of the South Platte River. The complex ages of these surfaces call into question any correlation of such surfaces based solely on their elevation above the modern channel.
© 2006 Elsevier B.V. All rights reserved.

Keywords: Cosmogenic nuclide; Incision; Terrace; Front Range; Denver basin

1. Introduction

The modern structure of the Rocky Mountain landscape in Wyoming and northern Colorado was determined during the Laramide Orogeny 80–50 Ma (e.g., Dickinson et al., 1988) by deep-seated thrusting

* Corresponding author. Tel.: +1 610 526 7971; fax: +1 610 526 5086.
E-mail addresses: criihima@brynmawr.edu (C.A. Riihimaki), robert.s.anderson@colorado.edu (R.S. Anderson), safran@lclark.edu (E.B. Safran), ddethier@williams.edu (D.P. Dethier), rfinkel@llnl.gov (R.C. Finkel), pbierman@uvm.edu (P.R. Bierman).

0169-555X/$ - see front matter © 2006 Elsevier B.V. All rights reserved.
doi:10.1016/j.geomorph.2006.01.035

that abutted crystalline basement rock of the ranges against easily eroded pre- and synorogenic sediments of intermontane basins. Subsequently, the topography of this region has further evolved in the absence of strong tectonic forcing. The modern high relief of the region formed during the late Cenozoic, as extensive channel incision formed deep canyons in the ranges and exhumed the basins (e.g., Epis and Chapin, 1975; Mears, 1993; Anderson et al., 2006). Remnant alluvial surfaces, high above modern streams within sedimentary basins, record past stream elevations during this late Cenozoic incision (Hunt, 1954; Scott, 1962, 1975; Madole, 1991; Chadwick et al., 1997). Understanding the timing and the mechanics of formation and preservation of these surfaces is a prerequisite to interpreting the timing and regional pattern of stream incision.

The Denver basin, just east of the Colorado Front Range, contains a series of Pleistocene pediments and strath terraces (henceforth called terraces or surfaces) that reflect periodic incision of, and lateral planation by, tributaries in response to downcutting of the South Platte River, the effective local base level (e.g., Hunt, 1954; Scott, 1962, 1975). Age constraints on these surfaces are limited to isolated ash deposits (e.g., Izett and Wilcox, 1982) and fossils (e.g., Scott, 1960) within the capping gravel deposits, and to semi-quantitative assessments of soil development (e.g., Scott, 1962; Birkeland et al., 1999; references cited in Shroba and Carrara, 1996). Terraces at the same elevation above base level are generally assumed to be isochronous (e.g., Reheis et al., 1991 and references therein), in contrast to mapping of Lava Creek B ash deposits that indicates regionally variable erosion rates since 640 ka (Dethier, 2001) and numerical modeling that suggests individual strath-terrace formation can span tens of thousands of years (Hancock and Anderson, 2002).

In this paper, we use concentrations measured in terrace alluvium of the in situ-produced terrestrial cosmogenic nuclides ^{10}Be and ^{26}Al (TCNs) to constrain the exposure ages and depositional histories of surfaces that abut the Front Range. These data allow us to assess the time span over which streams deposited and reworked the terrace alluvium, and therefore to constrain the spatial pattern of stream incision into the surfaces. Our results indicate that stream incision is spatially non-uniform and landscape morphology is non-steady in this region. We conclude by suggesting that the pattern of landscape evolution at the mountain front is a function of drainage area of the streams draining the Front Range.

2. TCN background

Production of ^{10}Be and ^{26}Al occurs through three main processes: nucleon spallation, negative muon capture and fast muon reactions. Each process has a distinctive extinction rate as a function of depth below the surface. The concentration of TCNs in sedimentary deposits therefore depends on both the initial exposure history of the sediment prior to deposition as well as the exposure and erosion history of the deposit after deposition (see Bierman, 1994; Gosse and Phillips, 2001). The concentration of ^{26}Al and ^{10}Be in quartz within a noneroding sedimentary deposit can be expressed as

$$N = N_{\mathrm{inh}} e^{-t/\tau} + \tau P(1 - e^{-t/\tau}) \quad (1)$$

where N_{inh} is the inherited concentration at the time of deposition, t is the time since deposition, τ is the mean life of the nuclide ($\tau_{26_{Al}} = 1.02 \pm 0.04$ Myr, Norris et al., 1983; $\tau_{10_{Be}} = 2.18 \pm 0.09$ Myr, Hofmann et al., 1987), and P is the elevation-, latitude- and depth-corrected production rate from nucleon spallation and muogenic processes (e.g., Granger and Smith, 2000). The production rate is approximated by

$$P = f_{\mathrm{sp}} P_{\mathrm{sp}} e^{-z/L_0} + f_{\mathrm{mu}} (P_{\mathrm{mu},1} e^{-z/L_1} + P_{\mathrm{mu},2} e^{-z/L_2} + P_{\mathrm{mu},3} e^{-z/L_3}) \quad (2)$$

where f_{sp} and f_{mu} are latitude and altitude correction factors for spallation and muogenic production; P_{sp} is the high-latitude, sea-level nucleon spallation production rate; $P_{\mathrm{mu},1}$, $P_{\mathrm{mu},2}$ and $P_{\mathrm{mu},3}$ are high-latitude, sea-level muogenic production rates; L_0, L_1, L_2 and L_3 are the attenuation length scales for each production rate; and z is the sample depth (Stone, 2000; Granger and Muzikar, 2001). The attenuation length scales each depend on the density ρ of the rock or sediment. Using this calculated production rate and assuming an inherited concentration and depth history for each sample, the exposure age of the deposit can be modeled (Eq. (1)). In some cases, depth profiles can allow for independent calculation of the inherited concentration (e.g., Anderson et al., 1996; Hancock et al., 1999; Perg et al., 2001).

3. Stream profiles and terrace morphology

We focus on extensive, well-preserved terraces along two tributaries of the South Platte River between Boulder and Golden, Colorado (Fig. 1). Coal and Ralston Creeks have relatively small drainage areas at the mountain front (44 and 55 km^2, respectively) and

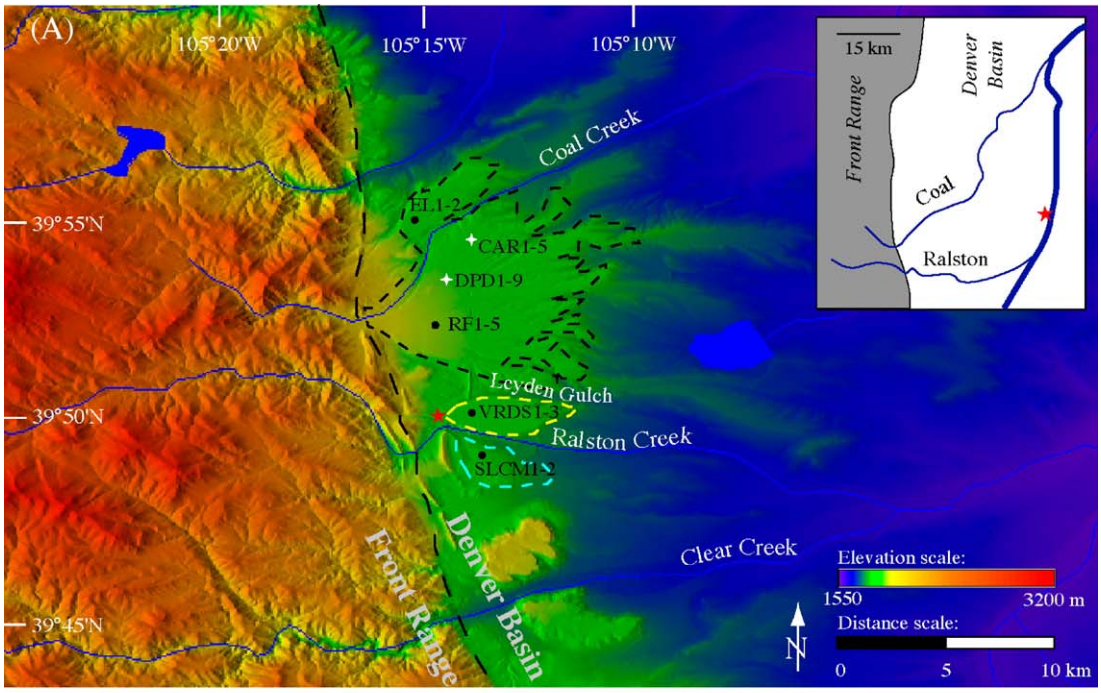

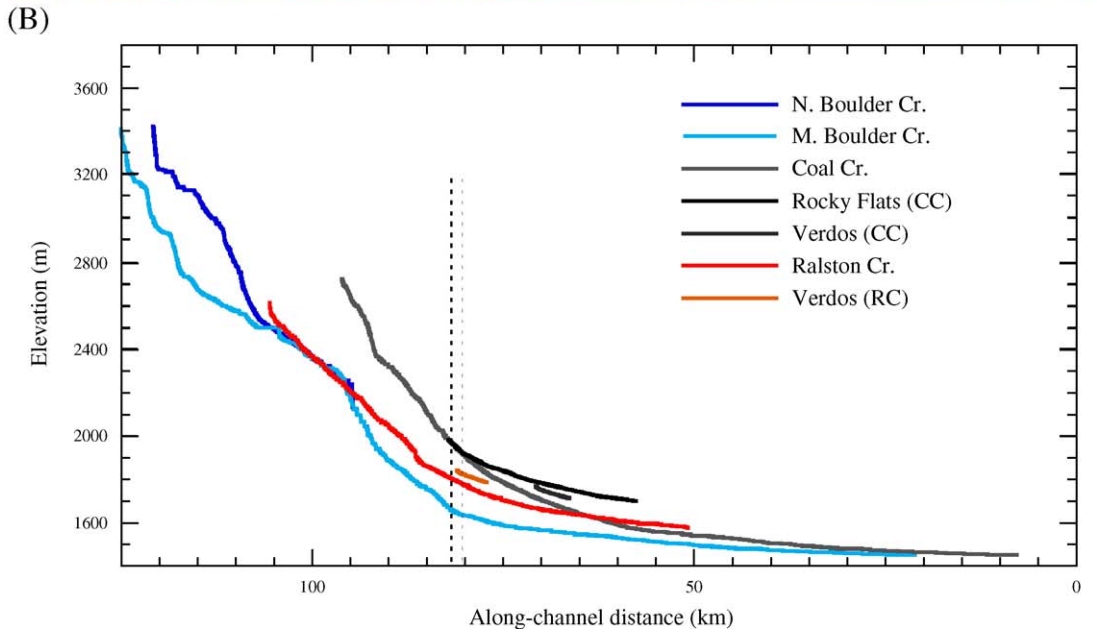

Fig. 1. (A) Shaded-relief map of the Rocky Flats region showing sample locations (circles indicate surface samples, crosses indicate depth profiles) and major surfaces (short dashes; black = Rocky Flats, yellow = Verdos, cyan = Slocum). Long dashes mark the boundary between the Front Range and Denver basin. Red star indicates the location of a Lava Creek B deposit above Ralston Creek. Inset map shows the course of each creek to their common junction along the South Platte River and the location of a Lava Creek B deposit above the South Platte River (red star in inset map). (B) Profiles of Coal, Ralston, and North and Middle Boulder Creeks; and profiles of Rocky Flats and Verdos along Coal Creek (CC) and Verdos along Ralston Creek (RC). Dashed line shows the boundary between the range and basin. The elevation of the streams at this boundary differs by ~300 m. The Ralston Creek profile at the mountain front has been interpolated across Ralston Reservoir.

exit the mountain front at relatively high elevations (1975 and 1800 m, respectively; Fig. 1B). Several nearby streams have larger drainage areas within the range and are more deeply incised into the mountain front. For example, Boulder Creek, 15 km to the north of Coal Creek, has a 250-km^2 drainage basin that extends

to the glaciated crest of the Front Range and exits the mountain front at 1650 m. Coal Creek merges with Boulder Creek 38 km downstream of the mountain front and with St. Vrain Creek 50 km downstream before entering the South Platte River 80 km downstream (Fig. 2). Ralston Creek merges with Clear Creek 20 km downstream of the mountain front and with the South Platte 32 km downstream. Thus, the Ralston channel network upstream of the confluence of St. Vrain Creek and South Platte River, including segments of Clear Creek and South Platte River, has a significantly larger drainage area than the Coal network upstream of the same point.

The Rocky Flats (RF) surface (Scott, 1960)–the most extensive high surface in this area (Shroba and Carrara, 1996)–is best preserved at the mouth of Coal Creek. This broadly concave surface projects into the Denver basin to an elevation ~100 m above the South Platte River (Scott, 1962). The existing eastern edge of the RF surface has been incised by up to 75 m. However, relief above several modern streams monotonically declines toward the mountain front, where the RF surface merges smoothly with the Coal Creek channel profile (Fig. 1B).

Lower, gravel-capped terraces in the Denver basin have been named the Verdos (VRDS), Slocum (SLCM), Louviers and Broadway surfaces (Scott, 1960). Two of the best-preserved examples are found between the RF surface and Ralston Creek, where the VRDS surface is ~45 m and the SLCM surface ~25 m above the creek (Fig. 1B).

The gravel caps of the RF, VRDS, and SLCM surfaces vary in thickness from 1 to 30 m because of relief on the underlying bedrock; typical gravel

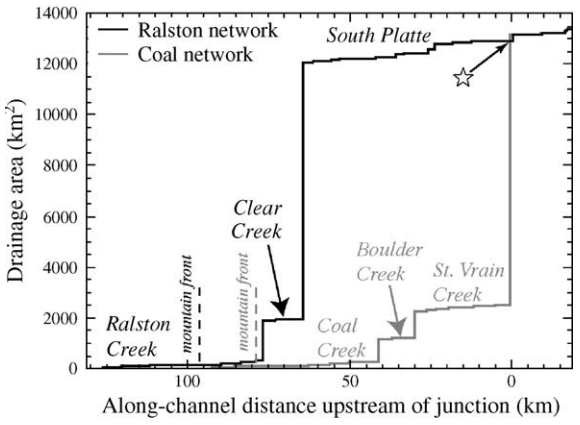

Fig. 2. Drainage areas of the Ralston (black) and Coal (gray) channel networks versus distance upstream of where the two networks merge (star). Dashed lines show the location of the mountain front along each network. Stepped increases in drainage area indicate the confluence of two streams.

thickness is 1–5 m (Shroba and Carrara, 1996). Despite the smooth topography of the RF surface, recent detailed mapping of the gravel thickness has revealed paleochannels filled with as much as 30 m of gravel (Knepper, 2005). The alluvium tends to be clast-supported and poorly sorted; clasts within the alluvium range in diameter from ~1 to 20 cm and boulders on the surface reach 75 cm. The RF alluvium is weathered and oxidized to depths that locally exceed 5 m and the upper several meters support a series of complex, strongly developed soils (Van Horn, 1976; Madole, 1991; Birkeland et al., 1999). Sharp, eroded contacts between buried soils and overlying sediment in this soil sequence suggest that the alluvial deposits have been modified by resurfacing events involving erosion and redeposition. Buried soils within the VRDS alluvium likewise illustrate long-term modification of the alluvium by Ralston Creek (Birkeland et al., 1999). Periodic burial by loess likely has occurred on the RF surface, as it has on other surfaces in the Rocky Mountain basins (e.g., Hancock et al., 1999). However, presently mappable loess deposits are >25 km east of the mountain front (Muhs et al., 1999).

4. Conceptual models of terrace dissection

The approximate timing of fluvial incision into the eastern portions of the RF surface can be estimated from constraints on the age of VRDS surfaces east of the field area. The gravels that cap these surfaces contain Lava Creek B ash and are therefore ~640 ka (inset of Fig. 1A; Scott, 1962; Izett and Wilcox, 1982; Shroba and Carrara, 1996). There is an additional Lava Creek B deposit north of Ralston Creek at the mountain front (Fig. 1A; Van Horn, 1976), but it has been reworked and deposited with alluvial fan sediment that has no clear age relationship with the neighboring VRDS alluvium (Birkeland et al., 1999). The elevations and ages of the VRDS gravel deposits along the South Platte River imply local incision rates of 50–100 m Ma^{-1} for the South Platte River since 640 ka (Izett and Wilcox, 1982; Dethier, 2001). Assuming the incision rates have persisted since the early Pleistocene, the eastern portion of the RF surface was likely incised and therefore abandoned at ~1–2 Ma based on its projected elevation 100 m above the South Platte River.

Incision by the South Platte River into the eastern part of the RF surface at 1–2 Ma does not necessarily indicate that Coal Creek began to incise into the western portion of the surface at that time. The spatial pattern of declining incision of Coal Creek into the RF surface toward the mountain front can be explained by: (i) one or more headward-propagating waves of incision that

have not yet reached the mountain front; or (ii) simultaneous incision along the length of terrace-traversing streams that has been more rapid in downstream reaches. The first scenario permits modification of capping gravel deposits close to the mountain front during incision of the eastern margin of the pediment, while the second scenario implies a more uniform date of surface abandonment. The complex series of buried soils within RF alluvium are consistent with the first scenario, but there are few additional constraints on the spatial pattern of Coal Creek incision. The spatial distribution of capping gravel ages, modeled using in situ-produced ^{26}Al and ^{10}Be, suggests age ranges for these presently undated surfaces delineating the pattern of pediment incision.

5. Sampling scheme

We sampled four sites on the RF surface, and one site each on the VRDS and SLCM surfaces (Fig. 1, Table 1) (surfaces mapped by Trimble and Machette, 1979). Sites on RF surface consisted of surface samples and depth profiles and ranged between 1.5 and 3.7 km from the mountain front (Fig. 1). The two depth profiles allowed us to examine the possibility of complex histories of the surface at each site.

Surface samples were collected from the outer rinds (<5 cm thick) of surface boulders. From the RF, VRDS and SLCM surfaces, we collected the outer rinds of 4, 3 and 2 boulders, respectively. Sample RF5 is an amalgamated sample of 30 pebbles, each 1–5 cm in diameter. Sample locations were sufficiently removed (>30 m) from the edges of the pediments and terraces that post-depositional mass wasting and fluvial erosion were negligible. We sampled upper surfaces of large, Precambrian quartzite boulders that showed no evidence of recent erosion; upwind sides were commonly ventifacted, indicating lack of boulder rotation. To minimize the likelihood that sampled rock was once buried by loess, all surface boulder samples were taken from >20 cm above the modern ground surface. Given the flatness of the topographic surfaces sampled and their distances from the range front, topographic shielding at our sample locations was negligible.

Depth profiles included a 4-m profile consisting of sand and pebbles (collected by D.P. Dethier; referred to as "DPD profile") and a 10-m profile consisting of gravel clasts 5–15 cm in diameter (collected by C.A. Riihimaki; referred to as "CAR profile"). Given the difficulty of excavating vertical exposures in gravel deposits, we opportunistically sampled profiles that were exposed in mining and engineering operations.

Table 1
Location, depth and TCN production-rate correction factors for each sample

Sample	Depth (m) [a]	Altitude (m)	Longitude (°W)	Latitude (°N)	f_{sp} [b]	f_{mu} [b]
Rocky Flats						
CAR1	9.60±1	1859	105.23	39.91	4.14	2.17
CAR2	7.00±1	1859	105.23	39.91	4.14	2.17
CAR3	6.30±1	1859	105.23	39.91	4.14	2.17
CAR4	1.60±1	1859	105.23	39.91	4.14	2.17
CAR5	0.00±1	1859	105.23	39.91	4.14	2.17
DPD1	3.76±0.3	1890	105.24	39.89	4.23	2.20
DPD2	2.96±0.3	1890	105.24	39.89	4.23	2.20
DPD3	2.36±0.3	1890	105.24	39.89	4.23	2.20
DPD4	1.96±0.3	1890	105.24	39.89	4.23	2.20
DPD5	1.56±0.3	1890	105.24	39.89	4.23	2.20
DPD6	1.06±0.3	1890	105.24	39.89	4.23	2.20
DPD7	0.61±0.3	1890	105.24	39.89	4.23	2.20
DPD8	0.36±0.3	1890	105.24	39.89	4.23	2.20
DPD9	0.13±0.3	1890	105.24	39.89	4.23	2.20
RF1	0.00±0.1	1934	105.25	39.87	4.36	2.24
RF2	0.00±0.1	1933	105.25	39.87	4.35	2.23
RF3	0.00±0.1	1933	105.25	39.87	4.35	2.23
RF4	0.00±0.1	1932	105.25	39.87	4.35	2.23
RF5	0.00±0.1	1932	105.25	39.87	4.35	2.23
EL1	0.00±0.1	1890	105.25	39.92	4.23	2.20
EL2	0.00±0.1	1890	105.25	39.92	4.23	2.20
Verdos						
VRDS1	0.00±0.1	1848	105.23	39.84	4.10	2.16
VRDS2	0.00±0.1	1835	105.23	39.84	4.06	2.15
VRDS3	0.00±0.1	1836	105.23	39.84	4.07	2.15
Slocum						
SLCM1	0.00±0.1	1793	105.22	39.82	3.94	2.11
SLCM2	0.00±0.1	1793	105.22	39.82	3.94	2.11

[a] Depth error from thickness of layer sample and human disturbance of surface.
[b] After Stone (2000).

The DPD profile was exposed temporarily during realignment of an irrigation canal, while the CAR samples were exposed during gravel mining operations. The original depths of the CAR samples are uncertain because the gravel-pit surface was reworked during mining. Based on the elevation of the top of the profile relative to adjacent, unmodified parts of the gravel cap, up to 2 m of surface gravel may have been removed. Samples CAR2 and CAR4 were collected from a single vertical exposure, while the other samples were collected from a stepped exposure on a different wall of the gravel pit, ~20 m away. Both exposures revealed significant weathering in the subsurface down to depths >4 m. We observed no evidence of significant bioturbation in either profile. We also observed no striking textural unconformities in the CAR profile and we therefore conclude that the

Table 2
Variables used in Eq. (2)

Variable	Value-^{10}Be	Value-^{26}Al
P_n [a]	5.0±0.3 atoms g^{-1} year^{-1}	30.4±1.9 atoms g^{-1} year^{-1}
$P_{mu,1}$ [b]	0.09 atoms g^{-1} year^{-1}	0.72 atoms g^{-1} year^{-1}
$P_{mu,2}$ [b]	0.02 atoms g^{-1} year^{-1}	0.16 atoms g^{-1} year^{-1}
$P_{mu,3}$ [b]	0.02 atoms g^{-1} year^{-1}	0.19 atoms g^{-1} year^{-1}
L_0 [b]	160/ρ cm	160/ρ cm
L_1 [b]	738/ρ cm	738/ρ cm
L_2 [b]	2688/ρ cm	2688/ρ cm
L_3 [b]	4360/ρ cm	4360/ρ cm

[a] From Stone (2000).
[b] From Granger and Muzikar (2001).

gravel at this location was deposited in several closely spaced events.

In contrast, changes in color and sand/gravel ratios in the DPD profile indicate that this profile contains at least two paleosols, the tops of which are at depths of 1.9 and 0.35 m. At depths <0.20 m, we observed little weathering, indicating that the gravel is relatively young and likely derived from minor slope wash during historic times. The accumulation of TCNs in this topmost layer probably occurred prior to deposition at this site, rather than in situ. We conclude that the DPD profile includes at least two major and one minor depositional event.

Based on the samples' field settings (Table 1), we can calculate the appropriate variables for Eq. (2) (Table 2). We assume that individual clasts are not eroding and that depth profiles undergo surface erosion only in rare events. We also assume that single clasts have a rock density of 2.7 g cm^{-3}, while gravel deposits have a bulk density of 1.89 g cm^{-3} (using a rock density of 2.7 g cm^{-3} and a porosity of 30%).

6. Laboratory methodology

For the DPD profile, samples were processed at the University of Vermont. These sediment samples were sieved to isolate the sand fraction (250–850 μm). For sample DPD9, pebbles with diameters <4 cm were crushed and added to the sand fraction so that sufficient quartz (9 to 40 g, μ=34 g) was available for analysis. Samples were processed for ^{10}Be and ^{26}Al using standard techniques including extraction of the aliquots for ICP-AES analysis of stable Al directly from HF solution before dry down (Bierman and Caffee, 2001). Yields for Be spikes averaged 98% for all samples and, for the two Al blanks associated with these samples, the Al yields were 100.7% and 98.9%. The DPD samples were spiked with 250 μg of Be carrier and variable amounts of Al carrier to ensure at least 2000 μg of Al were present for analysis. All accelerator mass spectrometric (AMS) analyses were made at Lawrence Livermore National Laboratory, are referenced to standards produced by K. Nishiizumi, and are corrected for ratios measured in blanks processed along with the samples. Measured ratios ranged from 1.3×10^{-12} to 7.4×10^{-12} for ^{10}Be/^{9}Be and 7.4×10^{-13} to 1.1×10^{-11} for ^{26}Al/^{27}Al. Blank subtractions were minimal, on average <1% of the measured ratios. The average, fully propagated uncertainty of the DPD profile analyses is 2.5% and 4.7% for ^{10}Be and ^{26}Al, respectively.

All other samples were processed at University of California at Santa Cruz. Samples EL1-2 were processed by G. Hancock in 1998, CAR samples were processed by C. Riihimaki in 2000, and RF, VRDS and SLCM samples were processed by C. Riihimaki in 2003. The samples were crushed and sieved to 250–500 μm (the initial grain sizes are given in Section 5). We used selective chemical dissolution to separate and purify 15–50 g quartz from this grain-size fraction (Kohl and Nishiizumi, 1992). We spiked samples with 0.25–0.5 mg of ^{9}Be and 1 mg of ^{27}Al. For samples processed in 2003, we extracted aliquots for ICP analysis of stable Al directly from HF solution before dry down; for earlier samples, aliquots were extracted after dry down. We measured stable Al concentrations by optical emission spectrometry (ICP-OES) and by mass spectrometry (ICP-MS) at University of California at Santa Cruz and assigned 5% error to these measurements. We used standard treatments of HF, HNO_3 and $HClO_4$, and separated Al and Be through ion exchange to prepare Be and Al targets for measurement on the Lawrence Livermore National Laboratory accelerator mass spectrometer. Measured ^{10}Be/Be and ^{26}Al/Al ratios were normalized to the ICN ^{10}Be (using a half-life of 1.5×10^{6} years) and the National Bureau of Standards ^{26}Al standards. Measured ratios ranged from 3.65×10^{-13} to 1.14×10^{-11} for ^{10}Be/^{9}Be and 1.04×10^{-14} to 1.57×10^{-11} for ^{26}Al/^{27}Al. Blank subtractions were minimal, on average <1% of the measured ratios, except for the Al blank subtraction of the CAR-profile measurements, which was 8%. The average, fully propagated uncertainty of the CAR-profile analyses is 5.5% and 16% for ^{10}Be and ^{26}Al, respectively. The average, fully propagated uncertainty of the surface-sample analyses is 5.2% and 6.0% for ^{10}Be and ^{26}Al, respectively.

7. Depth profiles

7.1. Results

In both depth profiles, concentrations generally decrease with depth (Table 3), as expected from the

Table 3
TCN concentrations for CAR and DPD profiles

Sample	[^{10}Be] (10^5 atoms/g)	[^{26}Al] (10^6 atoms/g)	[^{26}Al]/[^{10}Be]
CAR1	6.14±0.34	0.18±0.05	0.29±0.09
CAR2	4.03±0.22	1.07±0.21	2.66±0.54
CAR3	5.26±0.29	0.83±0.16	1.59±0.31
CAR4	9.59±0.53	3.47±0.25	3.62±0.33
CAR5	48.16±2.55	13.90±0.90	2.89±0.24
DPD1	7.76±0.25	3.28±0.15	4.23±0.24
DPD2	9.83±0.26	4.06±0.19	4.13±0.22
DPD3	10.50±0.24	4.05±0.21	3.86±0.22
DPD4	12.00±0.28	5.45±0.26	4.54±0.24
DPD5	13.10±0.30	6.72±0.32	5.13±0.27
DPD6	16.20±0.38	8.71±0.41	5.38±0.28
DPD7	23.70±0.70	12.10±0.56	5.11±0.28
DPD8	31.90±0.71	16.90±0.79	5.30±0.27
DPD9	26.40±0.63	13.90±0.64	5.27±0.27

decrease in TCN production rates with depth. The shallowest sample in the DPD profile is a notable exception, with significantly lower concentrations than the subjacent, deeper sample. The low concentrations in the topmost layer can be explained by relatively recent deposition, an interpretation that is consistent with the lack of weathering in this layer. The ratio R also decreases with depth, although this decrease within the DPD profile is not smooth, abruptly decreasing at a depth of ~2 m, the top of a paleosol. Shallow samples within the DPD profile have a ratio of ~5, while R in deeper samples is ~4. The CAR profile has higher ^{10}Be concentrations at shallow depths than the DPD profile, but lower concentrations at greater depths. R decreases from 3.62 to 1.59, anomalously low values suggesting that Al was not conserved during processing of the UCSC samples prior to 2003. We therefore interpret ages for this profile based only on the ^{10}Be concentrations.

7.2. Interpretation of depth profiles

The interpretation of exposure ages based on the profile concentrations requires a numerical model of gravel deposition and reworking. Gravel deposits on beveled bedrock surfaces are commonly assumed to have been emplaced in a single episode; rapid deposition is assumed to have been followed by a period of either stability (Hancock et al., 1999; Perg et al., 2001) or steady erosion (Wolkowinsky and Granger, 2004) until sample collection. In contrast, the presence of paleosols and the complicated ^{26}Al/^{10}Be ratio profile at the DPD site indicate a history that includes more than one depositional event. We explore a variety of depositional scenarios using a numerical model to calculate the expected TCN concentrations and ratios in each RF depth profile. For the model, we calculate the total surface production rates at the altitude and latitude of the sample sites to be 20.8–21.9 atoms g^{-1} year^{-1} for ^{10}Be and 126.6–133.3 atoms g^{-1} year^{-1} for ^{26}Al in quartz (Stone, 2000).

We present modeled TCN concentrations and ratios in the DPD profile for two scenarios: (i) a single episode of deposition followed by a long period of stability and (ii) an episode of deposition, a period of stability, stripping of the top layer of the deposit and deposition of new sediment, followed by a second period of stability. For each scenario, the near-surface ratio of ~5.3 requires that there has been very recent stripping of the surface as well. We determined the best overall fit for each profile by minimizing the reduced χ^2 value, in which the deviations from the fit were normalized using measurement uncertainties and were divided by the degrees of freedom. The timing and the amount of initial stripping and subsequent deposition, as well as the thickness of recent stripping, were varied systematically over more than 10,000 model runs. We did not attempt to include deposition of the shallowest sample in our model because it represents a relatively small-scale reworking of sediment that likely accumulated a significant concentration of TCNs prior to the reworking. We neglect this sample in assessing the model's fit. We generously assign errors of 15% to accommodate analytical errors (<5%) and uncertainty in model parameters (e.g., N_{inh}).

The one- and two-event models allow calculation of the inherited concentration N_{inh} and an initial

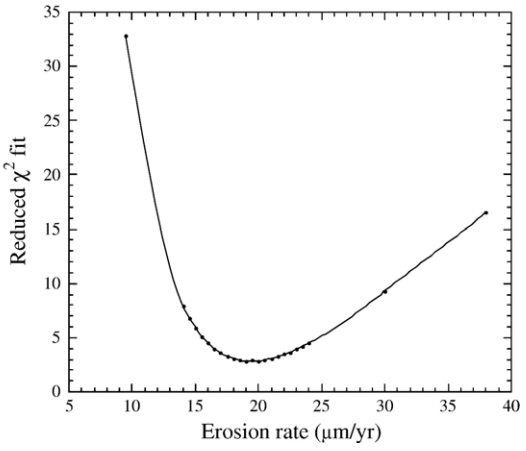

Fig. 3. Reduced χ^2 goodness-of-fit for the DPD profile versus assumed erosion rates in the Coal Creek basin for the two-event model. This profile independently constrains the basin-averaged erosion rate at 19 ±3 m Ma^{-1}.

concentration ratio because the model fit is sensitive to the inherited TCN concentrations (Fig. 3). An inherited ^{10}Be concentration of 9.9×10^5 atoms g^{-1} quartz and an initial concentration ratio ^{26}Al/^{10}Be of 6.05 produce the best fit to the data in both the one and two event models, values consistent with a basin-averaged erosion rate of 19±3 m Ma^{-1} at a mean elevation of 2500 m in the headwaters of the Coal Creek catchment. If the erosion rate is either doubled or halved, the model cannot adequately fit the concentration and R profiles simultaneously, resulting in high χ^2 values. The 19-m Ma^{-1} erosion rate is consistent with Holocene erosion rates of neighboring Deer Creek, 21.9 ±1.3 m Ma^{-1}, constrained by ^{10}Be concentrations in modern sediments (Dethier et al., 2002). The Deer Creek catchment is comparable to Coal Creek in size, elevation, and lithology. Modern Coal Creek sediment is unsuitable for a similar erosion rate analysis because significant human development in the headwaters has potentially affected the source of modern stream sediment and therefore ^{10}Be concentrations in modern sediment.

For the single-age scenario, the TCN data are best fit by a surface age of 780±115 ka, with 1.2±0.2 m of recent stripping. Although this model adequately reproduces the concentration profiles (Fig. 4A), it fails to reproduce the strong gradient in R and the distinct paleosol at 2-m depths (Fig. 4B). The two-event model (Figs. 4 and 5) succeeds in reproducing this feature. In the two-step model, we iteratively solve for two ages (for samples below and above 2-m depth) and the thickness of gravel removed during the two hypothesized stripping events. The best-fitting age of the lower gravels is 930±140 ka, while that for the upper 2 m is 550±80 ka. Because exposure of the paleosurface from 930 to 550 ka to cosmic rays would have generated TCN concentrations at the paleosurface significantly greater than inherited concentrations, a 3.1-m layer of gravel must have been removed prior to the second depositional event to prevent anomalously high nuclide concentrations at the 2-m horizon. Deposition without stripping the surface layer would have preserved high TCN concentrations at the 2-m horizon, with lower TCN values below and above that horizon. We calculate that the younger deposit was originally 3 m thick and was subsequently stripped by 1 m, possibly by loess deflation.

The history of the CAR profile is less well constrained because of the wide vertical spacing of samples and because Al likely was lost during laboratory analysis. Assuming that the deposited sediment had the same inherited concentrations as the DPD sediment, the very low ^{10}Be concentrations in deep samples suggest that the base of the profile is >1 Ma. Our best-fitting, single-age model (Fig. 6) suggests a surface age of 2.1±0.3 Ma with recent surface stripping of 1.7 m. This recent stripping could in fact be from the mining operations, but could alternatively be from erosion of a loess cap. Lack of

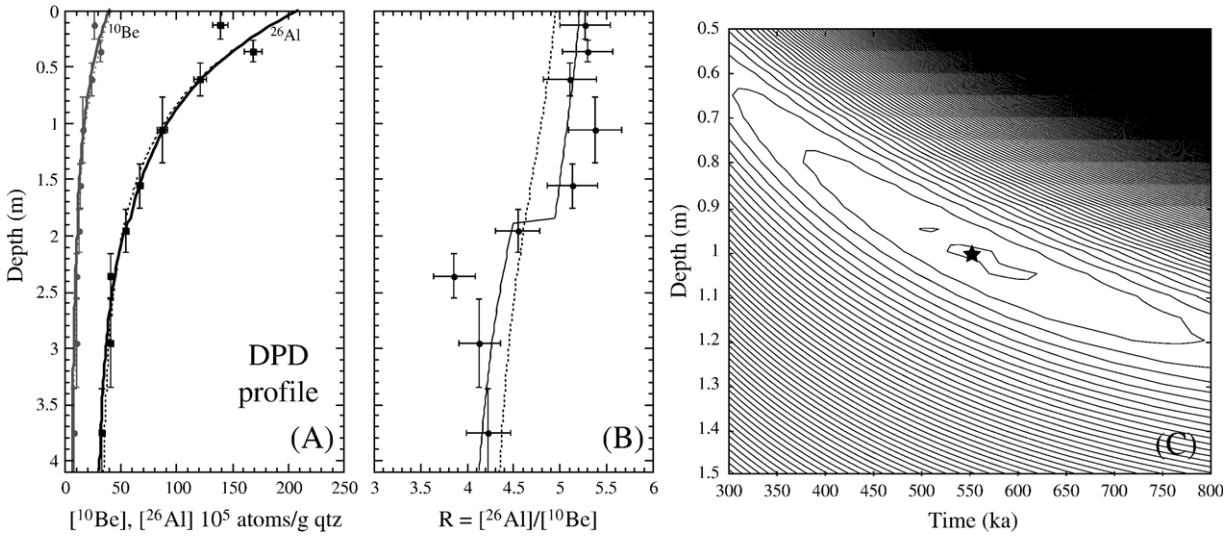

Fig. 4. (A) Concentrations of ^{10}Be (gray circles) and ^{26}Al (black squares) in the DPD profile with best-fitting profiles from the single-age model (dashed) and two-age model (solid). (B) ^{26}Al/^{10}Be data from DPD profile with best-fitting profiles from both models. (C) Contour plot showing reduced χ^2 goodness-of-fit for the DPD profile as a function of age of the shallow (<2-m depth) sediment and depth of stripping event at 0 ka. Best fit is shown with star. The contour interval is 1.0.

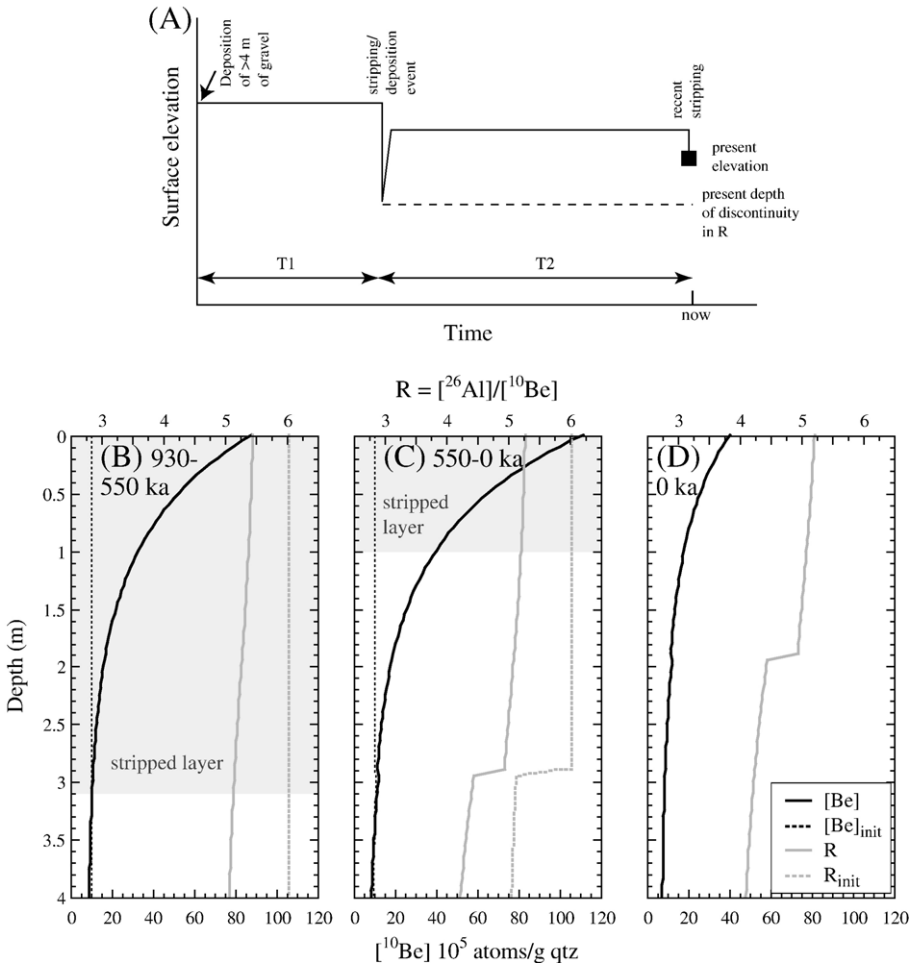

Fig. 5. (A) Schematic plot of the evolution of the RF surface elevation through time, showing two major depositional events and two stripping events. (B–D) Modeled evolution of ^{10}Be (black) and R (gray) for the DPD profile, with (B) deposition at 930 ka and stasis from 930 to 550 ka, (C) stripping of 3.1 m and deposition of 2.9 m at 550 ka followed by stasis from 550 to 0 ka, and (D) stripping of 1.0 m at 0 ka. Dashed lines show the initial values of ^{10}Be and R for each time period, while solid lines show values at the end of the period. Gray boxes show layer of gravel stripped at the end of each period.

reliable ^{26}Al measurements prevents the testing of more complex depositional histories at this site.

8. Surface clasts

8.1. Results

Concentrations of ^{10}Be in RF surface samples were 108±25 (10^5 atoms) g^{-1}, higher than ^{10}Be concentrations in VRDS and SLCM samples, which were 65±10 (10^5 atoms) g^{-1} and 53±5 (10^5 atoms) g^{-1}, respectively (Table 4). The concentration ratio ^{26}Al/^{10}Be (R) is 4.9±0.9 for RF samples, very similar to the VRDS and SLCM values of 5.0±0.7 and 5.2±0.6, respectively. There is no discernable trend in concentrations based on the height of the boulder sampled; RF5, the amalgamated-pebble sample had the second highest ^{10}Be concentration and an intermediate ratio, R. Except for the EL samples, we consider ^{26}Al measurements of these samples to be more reliable than the measurements for CAR profiles, because ICP aliquots were extracted prior to dry down for the surface samples.

8.2. Interpretation

The calculation of exposure ages of these surface samples requires knowledge of the inherited concentrations of TCNs and the exposure history of the samples. The DPD profile indicates that N_{inh} in the Coal Creek drainage is set on average by the basin-averaged erosion rate of 19±3 m Ma^{-1}. However, individual clasts sampled on the surface may have experienced a

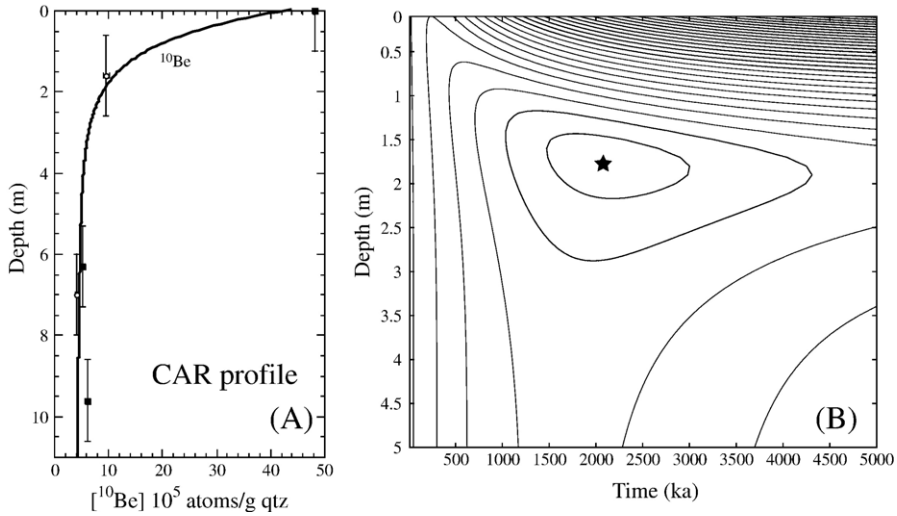

Fig. 6. (A) ^{10}Be concentrations in CAR profile with best-fitting model profile for single-age case. The samples came from two exposures (distinguished by open and closed symbols). (B) Contour plot showing reduced χ^2 goodness-of-fit for the CAR profile as function of age of the profile and depth of the recent stripping event. Best fit is shown with star. The contour interval is 0.1.

significantly higher or lower erosion rate prior to transport to and deposition at the mountain front, and therefore may have a significantly different value of N_{inh}. Individual clasts may likewise have been buried by varying thicknesses of sediment during their exposure history. To constrain the exposure ages and burial depths of the RF boulders, we model the evolution of ^{10}Be concentrations and R values in clasts buried at fixed depths ranging from 0 to 2 m (Fig. 7). We assume that the burial depths remain constant throughout the exposure of the clasts. We use three different basin-averaged erosion rates to achieve results that span a wide range of possible values of N_{inh}. By comparing the ^{10}Be concentrations and R values for RF samples to the model results, we determine a range of possible exposure ages and burial depths for the samples (Fig. 7).

Table 4
TCN concentrations and exposure ages for surface samples

Sample	[^{10}Be] (10^5 atoms g^{-1})	[^{26}Al] (10^6 atoms g^{-1})	[^{26}Al]/[^{10}Be]
Rocky Flats			
RF1	77.90±3.98	40.50±2.31	5.20±0.40
RF2	144.00±7.34	69.60±3.98	4.83±0.37
RF3	93.40±4.82	45.20±2.58	4.84±0.37
RF4	107.00±5.54	53.70±3.07	5.02±0.39
RF5	124.00±6.36	60.30±3.44	4.86±0.37
EL1	82.35±2.73	26.98±0.95	3.28±0.16
EL2	129.60±6.80	81.15±2.86	6.26±0.40
Average±1σ	108.32±25.15	53.92±18.30	4.90±0.88
Verdos			
VRDS1	54.25±2.80	23.74±1.35	4.38±0.34
VRDS2	67.09±3.48	31.65±2.04	4.72±0.39
VRDS3	74.44±3.86	42.95±2.45	5.77±0.44
Average±1σ	65.26±10.22	32.78±9.66	4.95±0.73
Slocum			
SLCM1	56.30±2.92	26.84±2.01	4.77±0.43
SLCM2	49.41±2.56	27.59±1.58	5.58±0.43
Average±1σ	52.86±4.87	27.21±0.53	5.17±0.58

Exposure ages of surface boulders and the amalgamated pebble sample from the RF surface based on ratios ^{26}Al/^{10}Be versus ^{10}Be concentrations range from 400 to 1000 ka, with average burial depths of <0.6 m (Fig. 7). The ages indicate that these boulders were deposited during the time when the DPD profile was deposited and modified (1–0.5 Ma). Because the RF samples were at 0-m depth at the time of collection, the sedimentary cover would have been removed recently, possibly by loess deflation. Our interpretation of recent stripping of sediment from above these samples is consistent with our interpretation that 1–2 m of sediment has been stripped recently from above the DPD and CAR profiles. The EL samples have ^{10}Be concentrations that fall within the range of RF values, indicating that these samples are likely the same age. However, because the ^{26}Al values are unreliable, we cannot fully analyze the depositional history of these samples.

The TCN concentrations of the few VRDS and SLCM samples are lower than they are in RF samples, consistent with the relative dating of these deposits as younger than the RF deposits. However, low R ratios of some of these samples and high R ratios for others indicate that their exposure history on these surfaces may be complex. Assuming that these samples have also

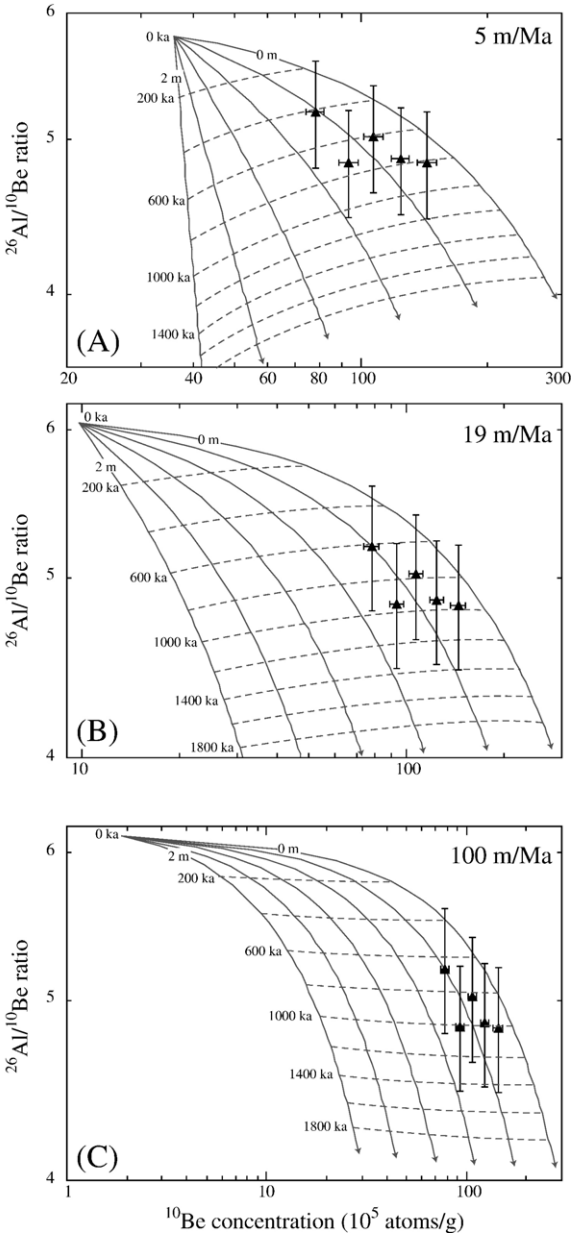

Fig. 7. Modeled evolution of ^{10}Be concentrations and ^{26}Al/^{10}Be ratios for clasts that are deposited on the RF surface with inherited concentrations set by basin-averaged erosion rates in the headwaters of (A) 5 m Ma^{-1}, (B) 19 m Ma^{-1} and (C) 100 m Ma^{-1}. Solid lines show the trajectories of clasts at fixed burial depths of 0–2 m (0.4-m intervals) and dashed lines indicate 200-kyr isochrons. RF samples (triangles) plot at 400–1000 ka and burial depths <0.6 m.

experienced a 19-m Ma^{-1} erosion rate in the Ralston Creek headwaters and that they were buried by 0.5 m of sediment after deposition at the mountain front, the exposure ages are ~500–1000 ka for the VRDS samples and ~600–700 ka for the SLCM samples. Assuming no burial, these ages drop to 200–400 ka and 200–300 ka, respectively.

9. Surface ages

We conclude that the alluvial history of the RF surface is complicated; no single age is appropriate for the entire deposit at some sites, nor may one assign a single age for the entire surface (Fig. 8A). Lava Creek B ash deposits that constrain the age of the VRDS surface and hence the incision rate of the South Platte River suggest incision into the eastern part of the RF surface began 1–2 Ma. Our modeling of the CAR profile, which is at our sample site farthest downstream along Coal Creek, suggests that alluvium in this region is ~2 Ma, corresponding to the timing of the South Platte River incision into the RF surface. The base of the DPD profile, 4 km upstream from the CAR site, appears to date from ~1 Ma, while the upper 2 m is ~0.5 Ma. This second event, which entails both stripping and redeposition of ~3 m of gravel, suggests that western portions of the RF surface continued to be reworked by

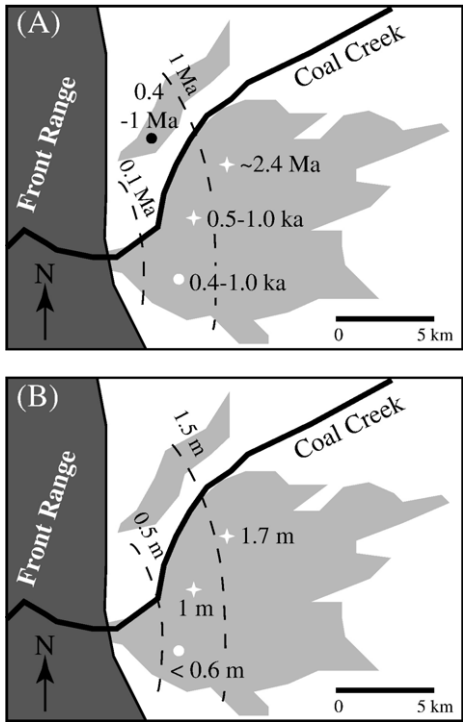

Fig. 8. Schematic maps of (A) alluvium ages and (B) thicknesses of recently stripped sediment on the Rocky Flats surface (see Fig. 1 for symbols). Dashed contour lines in (A) show the progressive incision of Coal Creek, with ages indicating the approximate time that streams began to incise at that location. Dashed contour lines in (B) show increasing sedimentary thicknesses away from the mountain front.

Coal Creek well after incision had abandoned sites farther east. Surface boulders on the western portion of the RF likewise have exposure ages consistent with deposition well after the South Platte River began incision into the distal reaches of the RF surface. These boulders could have been deposited during the same events that deposited the DPD profile. Finally, the modern Coal Creek remains unincised into the RF surface at the mountain front. These results and observations strongly suggest that the RF surface has been progressively abandoned from east to west, reflecting headward propagation of an incision wave along Coal Creek.

Modeling of burial histories of depth profiles and surface clasts suggests that the RF surface has been recently stripped of sediment, with thicknesses of stripped sediment increasing to the east, away from the mountain front (Fig. 8B). Although it is possible that human activity removed some sediment, particularly above the CAR profile, it is also possible that the RF surface was once covered by loess that has only recently been eroded. Loess deflation likely explains the stripping of sediment above the DPD profile and surface samples. The potential for recent anthropogenic and/or natural surface modification should therefore be considered when calculating the exposure ages of deposits within the Denver basin, even for deposits near the mountain front.

TCN concentrations in modern Coal Creek sediment (Dethier et al., 2002) and our calculated inherited concentrations from the DPD profile indicate that the Coal Creek catchment upstream of the RF surface has a significantly lower average erosion rate ($\sim$20 m Ma^{-1}) than local rates of stream incision by the South Platte River (50–100 m Ma^{-1}; Dethier, 2001). These results strongly suggest that the Front Range–Denver basin region is not a steady-state landscape (Willett and Brandon, 2002) but is evolving transiently, with highest erosion rates in the basin (Anderson et al., 2006). This is consistent with a model of stream incision in which waves of incision propagate upstream from the basin into the range, with the rate of propagation tied to hydrographic characteristics and size of individual tributaries. For the Coal Creek catchment, the incision has yet to propagate into the Front Range, resulting in a steady, low erosion rate of the headwaters since at least 1 Ma.

The incision history of Ralston Creek remains relatively unconstrained, but further dating of the VRDS and SLCM surfaces should indicate whether Ralston Creek has also experienced headward incision. Given that Ralston Creek has incised 150 m deeper at the mountain front than Coal Creek, Ralston Creek appears to have a greater ability to incise than Coal Creek at the mountain front. The more rapid incision by Ralston Creek than by Coal Creek may be the result of Ralston's 20% larger drainage area at the mountain front and consistently larger drainage area downstream (Fig. 2). This result is consistent with stream incision models in which stream power, which is proportional to drainage area, controls the rate of erosional-wave propagation (e.g., Tucker and Whipple, 2002). An erosional wave beginning at the common downstream points of the Coal and Ralston Creek networks (Fig. 2) would propagate more rapidly upstream along the Ralston Creek network because of its higher discharge, while the wave would propagate relatively slowly along the Coal Creek network. This effect is further enhanced if there exists a threshold of stream power (hence of drainage area) required for channel incision, effectively making the relationship between incision and basin area nonlinear for small drainage areas. Other possible explanations include subtle interbasin differences in lithology, precipitation patterns, and sediment transport.

10. Conclusions

TCN-based ages of the Rocky Flats, Verdos and Slocum surfaces may be explained by differential incision of tributaries in response to an eroding trunk stream. The profiles of streams draining the Front Range and Denver basin are transiently adjusting to the South Platte River that began incising into the eastern portion of the RF surface $\sim$1–2 Ma. Upstream propagation of incision waves causes diachronous abandonment of pediments near the mountain front, suggesting that no single age is appropriate for these extensive surfaces. Modeling of TCN depth profiles suggests that individual sites have complex depositional histories likely involving multiple depositional and stripping events. Because the time of abandonment of a given surface is determined by the power of its associated stream, surfaces at the same elevation above two different streams should not necessarily have the same age. Finally, as a corollary to these observations, we note that the persistence of an extensive remnant of the RF surface results from the small area and thus low stream power of Coal Creek.

Acknowledgements

This work was supported by a grant from the National Science Foundation (EAR-0003604), an NSF Graduate Student Fellowship (to CAR) and a University

of California Presidential Postdoctoral Fellowship (to EBS). LLNL work was done under the auspices of the U.S. Department of Energy under Contract No. W-7405-Eng-48. We thank Stephanie Kampf, Greg Stock, Mary Elizabeth Smith, Jennifer Ha, Graham Gilbert, Niels Zellers, Taylor Schildgen and Marc Caffee for their assistance. Comments by Darryl Granger, Noah Snyder and two anonymous reviewers greatly improved this manuscript.

References

Anderson, R.S., Repka, J.L., Dick, G.S., 1996. Explicit treatment of inheritance in dating depositional surfaces using in situ Be-10 and Al-26. Geology 24 (1), 47–51.

Anderson, R.S., Riihimaki, C.A., Safran, E.B., MacGregor, K.R, 2006. Facing reality: late Cenozoic evolution of smooth peaks, glacially ornamented valleys and deep river gorges of Colorado's Front Range. In: Willett, S.D., Hovius, N., Brandon, M.T., Fisher, D.M. (Eds.), Tectonics, Climate, and Landscape Evolution. Geological Society of America Special Publication, vol. 398. Geological Society of America, Boulder, CO. Chapter 25.

Bierman, P.R., 1994. Using in situ produced cosmogenic isotopes to estimate rates of landscape evolution: a review from the geomorphic perspective. Journal of Geophysical Research 99 (B7), 13885–13896.

Bierman, P.R., Caffee, M.W., 2001. Slow rates of rock surface erosion and sediment production across the Namib Desert and escarpment, southern Africa. American Journal of Science 301, 326–358.

Birkeland, P.W., Miller, D.C., Patterson, P.E., Price, A.B., Shroba, R.R., 1999. Soil-geomorphic Relationships Near Rocky Flats, Boulder and Golden, Colorado Area, with a Stop at the Pre-Fountain Formation Paleosol of Wahlstrom (1948). Geological Society of America Field Trip, vol. 18. 13 pp.

Chadwick, O.A., Hall, R.D., Phillips, F.M., 1997. Chronology of Pleistocene glacial advances in the central Rocky Mountains. Geological Society of America Bulletin 109 (11), 1443–1452.

Dethier, D.P., 2001. Pleistocene incision rates in the western United States calibrated using Lava Creek B tephra. Geology 29 (9), 783–786.

Dethier, D.P., Ouimet, W.B., Bierman, P.R., Finkel, R.C., 2002. Long-term erosion rates derived from 10Be in sediment from small catchments, northern Front Range and southern Wyoming. Abstracts with Programs - Geological Society of America 34 (6), 409.

Dickinson, W.R., Klute, M.A., Hayes, M.J., Janecke, S.U., Lundin, E.R., McKittrick, M.A., Olivares, M.D., 1988. Paleogeographic and paleotectonic setting of Laramide sedimentary basins in the central Rocky-Mountain region. Geological Society of America Bulletin 100 (7), 1023–1039.

Epis, R.C., Chapin, C.E., 1975. Geomorphic and tectonic implications of the post-Laramide, late Eocene erosion surface in the southern Rocky Mountains. In: Curtis, B.F. (Ed.), Cenozoic History of the Southern Rocky Mountains. Geological Society of America Memoir, vol. 144, pp. 45–74. Geological Society of America, Boulder, CO.

Gosse, J.C., Phillips, F.M., 2001. Terrestrial in situ cosmogenic nuclides: theory and application. Quaternary Science Reviews 20 (14), 1475–1560.

Granger, D.E., Muzikar, P.F., 2001. Dating sediment burial with in situ-produced cosmogenic nuclides: theory, techniques, and limitations. Earth and Planetary Science Letters 188, 269–281.

Granger, D.E., Smith, A.L., 2000. Dating buried sediments using radioactive decay and muogenic production of Al-26 and Be-10. Nuclear Instruments and Methods in Physics Research. Section B, Beam Interactions with Materials and Atoms 172, 822–826.

Hancock, G.S., Anderson, R.S., 2002. Numerical modeling of fluvial strath-terrace formation in response to oscillating climate. Geological Society of America Bulletin 114 (9), 1131–1142.

Hancock, G.S., Anderson, R.S., Chadwick, O.A., Finkel, R.C., 1999. Dating fluvial terraces with Be-10 and Al-26 profiles: application to the Wind River, Wyoming. Geomorphology 27 (1–2), 41–60.

Hofmann, H.J., Beer, J., Bonani, G., Vongunten, H.R., Raman, S., Suter, M., Walker, R.L., Wolfli, W., Zimmermann, D., 1987. Be-10 —half-life and AMS-standards. Nuclear Instruments and Methods in Physics Research. Section B, Beam Interactions with Materials and Atoms 29 (1–2), 32–36.

Hunt, C.B., 1954. Pleistocene and recent deposits in the Denver area, Colorado. U.S. Geological Survey Bulletin 996-C, 91–140.

Izett, G.A., Wilcox, R.E., 1982. Map showing localities and inferred distributions of the Huckleberry Ridge, Mesa Falls, and Lava Creek ash beds (Pearlette family ash beds) of Pliocene and Pleistocene age in the western United States and southern Canada. U.S. Geological Survey Miscellaneous Investigations Series Map I-1325.

Knepper, D.H., 2005. Bedrock erosion surface beneath the Rocky Flats alluvial fan, Jefferson and Boulder Counties, Colorado. The Mountain Geologist 42 (1), 1–10.

Kohl, C.P., Nishiizumi, K., 1992. Chemical isolation of quartz for measurement of in situ-produced cosmogenic nuclides. Geochimica et Cosmochimica Acta 56 (9), 3583–3587.

Madole, R.F., 1991. Quaternary geology of the northern Great Plains: Colorado Piedmont section. In: Morrison, R.B. (Ed.), Quaternary Nonglacial Geology: Conterminous U.S. Geological Society of America The Geology of North America K-2, Boulder, CO, pp. 456–462.

Mears Jr., B., 1993. Geomorphic history of Wyoming and high-level erosion surfaces. In: Snoke, A.W., Steidtmann, J.R., Roberts, S.M. (Eds.), Geology of Wyoming. Geological Survey of Wyoming Memoir, vol. 5, pp. 608–626.

Muhs, D.R., Aleinikoff, J.N., Stafford, T.W., Kihl, R., Been, J., Mahan, S.A., Cowherd, S., 1999. Late Quaternary loess in northeastern Colorado: Part I. Age and paleoclimatic significance. Geological Society of America Bulletin 111 (12), 1861–1875.

Norris, T.L., Gancarz, A.J., Rokop, D.J., Thomas, K.W., 1983. Half-life of Al-26. Journal of Geophysical Research 88, B331–B333.

Perg, L.A., Anderson, R.S., Finkel, R.C., 2001. Use of a new Be-10 and Al-26 inventory method to date marine terraces, Santa Cruz, California, USA. Geology 29 (10), 879–882.

Reheis, M.C., Palmquist, R.C., Agard, S.S., 1991. Quaternary history of southern and central Rocky Mountain basins: Bighorn basin. In: Morrison, R.B. (Ed.), Quaternary Nonglacial Geology: Conterminous U.S. Geological Society of America The Geology of North America K-2, pp. 409–416.

Scott, G.R., 1960. Subdivision of the Quaternary alluvium east of the Front Range near Denver, Colorado. Geological Society of America Bulletin 71, 1541–1543.

Scott, G.R., 1962. Geology of the Littleton Quadrangle, Jefferson, Douglas, and Arapahoe Counties, Colorado. U.S. Geological Survey Bulletin 1121-L, 1–53.

Scott, G.R., 1975. Cenozoic surfaces and deposits in the southern Rocky Mountains. In: Curtis, B.F. (Ed.), Cenozoic History of the Southern Rocky Mountains. Geological Society of America Memoir, vol. 144, pp. 227–248. Geological Society of America, Boulder, CO.

Shroba, R.R., Carrara, P.E., 1996. Surficial Geologic Map of the Rocky Flats Environmental Technology Site and Vicinity, Jefferson and Boulder Counties, Colorado. U.S. Geological Survey.

Stone, J.O., 2000. Air pressure and cosmogenic isotope production. Journal of Geophysical Research-Solid Earth 105, 23753–23759.

Trimble, D.E., Machette, M.N., 1979. Geology of the Greater Denver Area, Front Range Urban Corridor, Colorado. U.S. Geological Survey.

Tucker, G.E., Whipple, K.X., 2002. Topographic outcomes predicted by stream erosion models: sensitivity analysis and intermodel comparison. Journal of Geophysical Research-Solid Earth 107 (B9) (art. no.-2179).

Van Horn, R., 1976. Geology of the golden quadrangle, Colorado. U.S. Geological Survey Professional Paper 872 (116 pp.).

Willett, S.D., Brandon, M.T., 2002. On steady states in mountain belts. Geology 30 (2), 175–178.

Wolkowinsky, A.J., Granger, D.E., 2004. Early Pleistocene incision of the San Juan River, Utah, dated with Al-26 and Be-10. Geology 32, 749–752.